Perpendicular Magnetic Recording: Writing Process

In this article, a detailed overview of the methodology to design a write transducer for recording onto perpendicular media at areal densities beyond 1 Tbit/in.2 is presented. The two basic modes of perpendicular recording, single-layer recording media in combination with a ring type head and double-layer recording media with a soft underlayer in combination with a single pole head, are compared with each other theoretically and experimentally.

The following article appeared in the Journal of Applied Physics, Volume 95, Number 9, 1 May 2004 and may be found at http://scitation.aip.org/.

APPLIED PHYSICS REVIEWS—FOCUSED REVIEW

Perpendicular magnetic recording: Writing process

S. Khizroev[a)]
Center for Nanoscale Magnetic Devices, Florida International University, Miami, Florida 33174

D. Litvinov
Center for Nanomagnetic Systems, University of Houston, Houston, Texas

(Received 31 July 2003; accepted 11 February 2004)

In this article, a detailed overview of the methodology to design a write transducer for recording onto perpendicular media at areal densities beyond 1 Tbit/in.^{2} is presented. The two basic modes of perpendicular recording, single-layer recording media in combination with a ring type head and double-layer recording media with a soft underlayer in combination with a single pole head, are compared with each other theoretically and experimentally. Moreover, perpendicular recording is compared to longitudinal recording from the perspective of the writing process. The system efficiency is redefined for perpendicular recording to take into account the critical role of the soft underlayer. The effects of using ''soft'' magnetic shields around the trailing pole are analyzed. It is shown that at least a factor of 2 increase in the field can be obtained at areal densities beyond 500 Gbit/in.^{2} if shields are used. Such an open issue as the skew angle sensitivity in perpendicular recording is analyzed. It is shown that using soft magnetic shields around the trailing pole substantially improves the skew angle sensitivity. Moreover, using shields substantially improves the system efficiency and to some degree fulfills the role of the soft underlayer in perpendicular recording. [DOI: 10.1063/1.1695092]

TABLE OF CONTENTS

I. INTRODUCTION

After fierce struggles to extend the life of longitudinal magnetic recording as the main technology for another couple of years, the data storage industry is finally coming to terms with reality. Reality says that the areal density in cutting-edge laboratory demonstration systems is limited by thermal instabilities in the longitudinal magnetic media.[1] Recent high areal density demonstrations of perpendicular re-

[a)]Electronic mail: khizroev@fiu.edu

cording clearly demonstrate the strong interest of the data storage industry in this alternative technology today.[2–5] Compared to the conventional longitudinal recording mode, it is believed that perpendicular recording is capable of deferring the superparamagnetic limit to a substantially higher areal density due to the thicker recording layer and/or the use of a soft underlayer (SUL).[6] Although perpendicular recording is certainly the closest alternative to conventional technology, its novelty also brings up new issues, not ever encountered in longitudinal recording. These issues have to be well understood before the technology can be fully and most efficiently implemented.[9,10] Major questions related to perpendicular media and perpendicular playback and writing heads have been previously considered.[14,22,23,26,32] However, relatively little attention has been given to the writing process at areal densities beyond 100 Gbit/in.[2].[20] For example, the role of soft magnetic shields in the writing process is still an unresolved: although the use of soft shields around the main pole of the writing head certainly increases the field gradient, its influence on the magnitude of the recording field is still controversial. Another fundamental question is the role of the soft underlayer in the writing process. These and many other questions associated with the writing process need to be considered altogether for the most efficient design of the write head. Therefore, the intention of this article is to analyze the writing process in perpendicular recording from the global perspective of maximizing the achievable areal density.

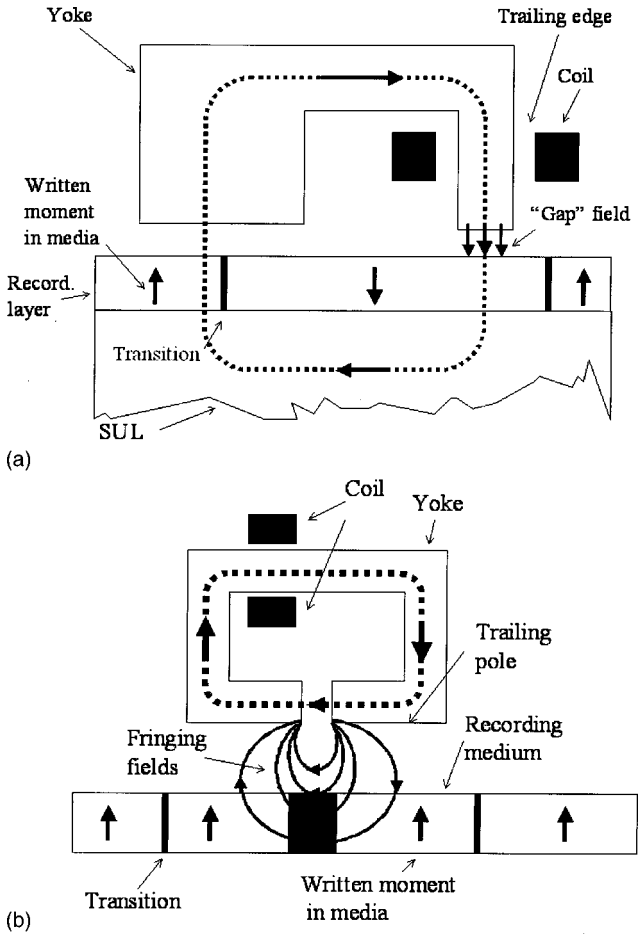

FIG. 1. Diagram showing a cross section of the side of a perpendicular system of (a) the first mode, including a SPH and a double-layer medium with a SUL, and (b) the second perpendicular mode, including a RH and a single-layer recording medium.

II. DIFFERENT MODES OF PERPENDICULAR RECORDING

There are two basic modes of perpendicular recording.[7] The first mode utilizes a single pole head (SPH) for recording onto a double-layer perpendicular medium consisting of a recording layer and a SUL, as shown in a diagram in Fig. 1(a).[8] As described below, the use of the SUL is one of the most critical factors contributing to one of the best-known advantages of perpendicular recording, which is the ability to generate a recording field of the order of $4\pi M_s$, where M_s is the saturation magnetization for the recording head material.[9,10] For comparison, in conventional recording, the maximum longitudinal recording field generated by a ring head (RH) is approximately $2\pi M_s$.[11] The ability to generate a stronger field makes it feasible to record on a medium with higher coercivity, which in turn further defers the superparamagnetic limit to a higher areal density.[12] The second mode utilizes a regular RH for recording onto a single-layer perpendicular medium, as shown in a diagram in Fig. 1(b). Although, the first mode is more widely exploited due to the advantages of the SUL, it is still reasonable to start with the description of the second mode, because the latter is fairly similar to the conventional longitudinal mode and, therefore, is going to be a good transitional step towards development of a structured theory of perpendicular recording. Both the longitudinal recording mode and the second perpendicular recording mode rely on the utilization of a ring head along with a medium without a soft underlayer. Through a comparison of these two recording modes, some of the critical features of perpendicular recording can be made fairly apparent.

Besides the two basic modes, in some cases, some kind of an intermediate mode, e.g., a RH and a medium with a SUL, or a SPH or a RH and a medium with a tilted magnetization with or without a SUL, can also be preferred, as discussed below. Moreover, it is shown that substantial modifications to basic head structures are required for the ability to record at densities beyond 1 Tbit/in.[2] In the following, advantages and issues associated with different recording modes are discussed in detail.

A. Second recording mode: Ring head and a perpendicular medium without a soft underlayer

As mentioned above, the second mode of perpendicular recording, which uses a conventional longitudinal ring head and a medium without a SUL, still remains an arena of exploration because of its resemblance to the conventional longitudinal mode and the lack of the ''not-yet-understood peculiarities'' of the SUL in the first mode.[9] A diagram showing a conventional longitudinal system is shown in Fig. 2(a). The only structural difference between the second perpendicular mode and the conventional longitudinal mode is in the me-

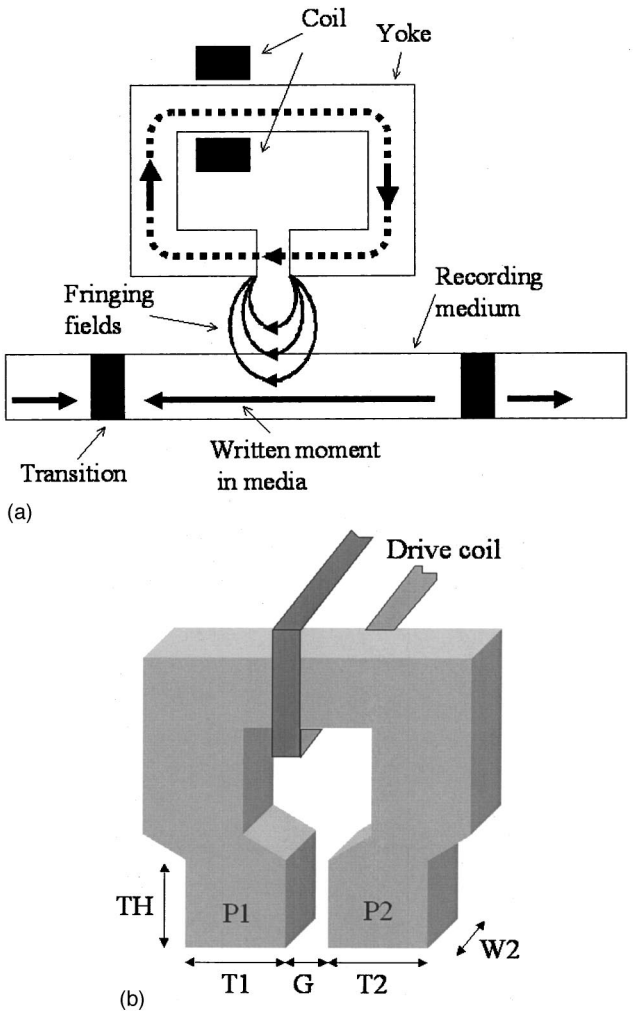

FIG. 2. Diagram showing (a) a cross section of the side of a typical longitudinal system, including a RH and a recording medium. (b) 3D schematic diagram of a RH.

dium magnetization orientation: the magnetization is in the plane and perpendicular to the disk plane for the longitudinal and perpendicular modes, respectively. Also, in the perpendicular mode, the medium's ''easy'' axis is ideally aligned in one direction (in the direction perpendicular to the disk plane), while in the longitudinal mode, the ''easy axes'' are randomly oriented in the disk plane.[13]

Because the RH is a critical part of longitudinal recording, a more detailed diagram of a conventional RH is shown in Fig. 2(b). Although, in most practical cases, the leading pole, P1, is typically substantially wider than the trailing pole, P2, here in Sec. II A, the assumption that both poles, P1 and P2, have the same thickness, $T1 = T2$, is used for simplicity to explain the key issues. Because the actual recording takes place near the trailing edge of the gap length, the effective track width is predominantly determined by the width of the trailing pole, W2, and does not strongly depend on the width of the leading pole.[14] Moreover, in the past, some recording head manufacturing companies, for example, ReadRite Corporation, did utilize a ring head with identical leading and trailing poles of the type shown in Fig. 2(b).[15] Using a specially developed magnetic force microscopy

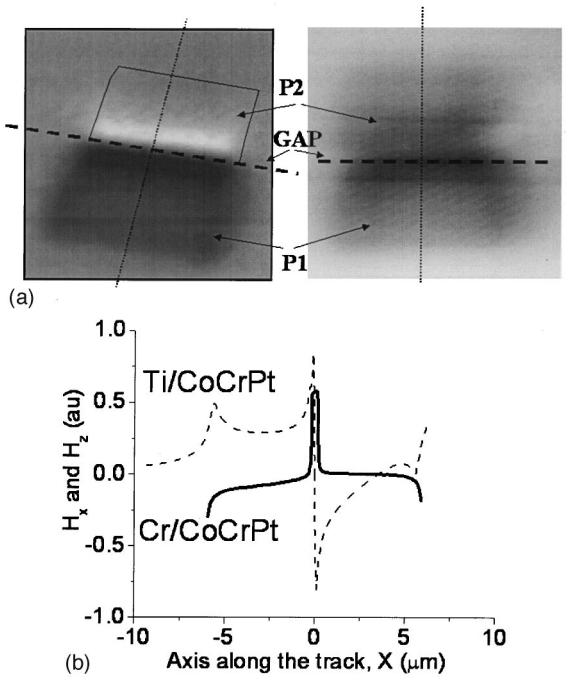

FIG. 3. (a) MFM images of the perpendicular and longitudinal field profiles taken at the ABS of a RH with 200 nm gap length. (b) Cross sections of these field profiles taken along the center line in the track direction.

(MFM) technique to separately measure individual components generated by such a RH, the perpendicular and longitudinal field profiles at the air-bearing surface (ABS) of such a RH were directly measured, as shown in Fig. 3(a).[16] The cross sections of these field profiles along the center line in the track direction are shown in Fig. 3(b).

In general, the RH structure has been widely studied in association with longitudinal recording, and there is plenty of literature which contains more detailed information about the RH design. In this work, the authors only discuss the aspects of RH design, which are of interest for perpendicular recording.

Before going into details of the head design analysis, it is worth recalling that, traditionally, the Karlqvist two-dimensional (2D) model has been utilized for describing the magnetic properties.[17] However, today, as the areal density reaches the point at which the track width becomes fairly small, 2D calculations cannot give sufficient accuracy. Therefore in this article, results of three-dimensional (3D) calculations made with boundary element model (BEM)-based commercial field solver Amperes are shown.[18]

1. Gap length dependence

The 3D calculated along-the-track (X-) and perpendicular (Z-) field components for a RH without a SUL at saturation for a set of four values of gap length, 30, 70, 150, and 500 nm, are shown in Figs. 4(a)–4(d), respectively. In these calculations, the value for the flying height was 5 nm, and the track width and the pole thickness were modeled to be 200 and 500 nm, respectively. Nevertheless, the efficiency depends on the gap length exactly as in longitudinal recording.[11,19] The dependence of the system efficiency on the gap length is reflected in the saturation current depen-

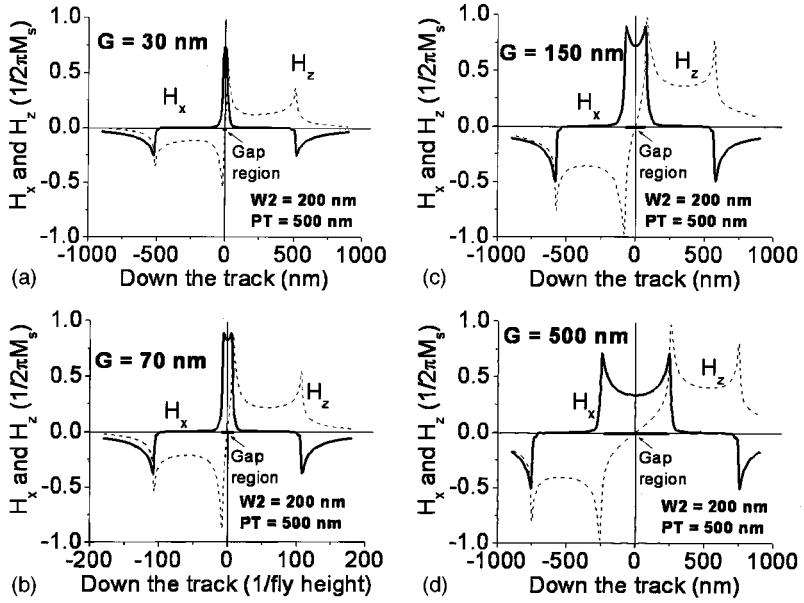

FIG. 4. Longitudinal and perpendicular field components vs the distance down the track for a RH with track width of 200 nm and pole thickness of 500 nm at four values of the gap length: (a) 30, (b) 70, (c) 150, and (d) 500 nm.

dence on the gap length, as shown in Fig. 5. The normalization factor (NF) necessary for determining the exact drive current value depends on specific head parameters, including its dimensions and the location of the drive coil with respect to the ABS.[19] The saturation current is determined as the current at which the recording field under the gap center at a 5 nm flying height starts to saturate. Going back to the description in Figs. 4(a)–4(d), with a gap length of 70 nm, the parameters chosen approximately correspond to areal density of 50 Gbit/in.[2]

Although, in practice, both field components, in plane and perpendicular, simultaneously influence each recording event, ideally, the perpendicular and longitudinal field components reflect the perpendicular and longitudinal recording modes, respectively. From the plots, it can be seen that the longitudinal field component is fairly well localized in the gap region. In this case, the field near the trailing edge of the gap produces the recording. As a result, by having the gap length sufficiently small, a fairly sharp field profile and fairly large areal densities can be produced. However, there is a limit to reducing the gap length. As the efficiency increases with reduction of the gap, less flux leaks out through the gap region, thus resulting in a weaker recording field. Eventually, the recording field becomes too small to overcome the medium's coercivity field. For example, in this particular case, this trade-off value of the gap, below which the longitudinal field component starts to drop, is in the vicinity of the 70 nm value, as seen from Figs. 4(a)–4(d). The trade-off value is mostly determined by the flying height and the track width. The scenario is different for the perpendicular field component, for which a fairly large value can be noted far beyond the gap region. As a result, in this case, recording is produced not by the field in the immediate vicinity of the gap region, but rather by the field near the trailing edge of the trailing pole, as long as the field near the trailing edge is larger than the coercivity field.[20] Also, it can be noted that the perpendicular field component at saturation even increases as the gap length is increased in the range considered. This is caused by the reduction of the longitudinal field contribution to the net flux as the gap increases, thus making the net field predominantly perpendicular. It can be noted that, unlike in longitudinal recording, the maximum field and the trailing field gradient are defined not only by the physical gap length but also to a substantial degree by the trailing pole tip geometry.

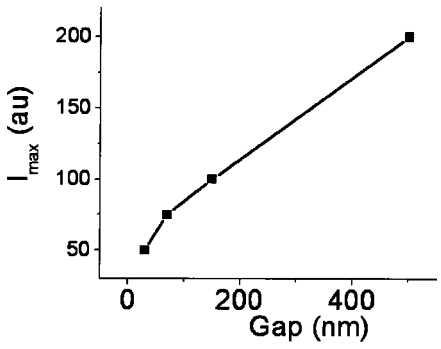

FIG. 5. Maximum field current vs the gap length.

However, for the both systems, the efficiency depends fairly strongly on the gap length because of the use of a RH. For any recording mode for which a RH is utilized with a medium without a SUL, transitions are produced by the fields which fringe out from the gap of the "closed" magnetic loop of the RH.[21] In other words, the gap region becomes a part of the magnetic flux loop, and therefore the efficiency of the loop strongly depends on the gap region. The dependence of the efficiency on the gap length is proportional to the dependence of the saturation current on the gap length. Assuming that the saturation current is defined as the current at which the longitudinal field at the center of the

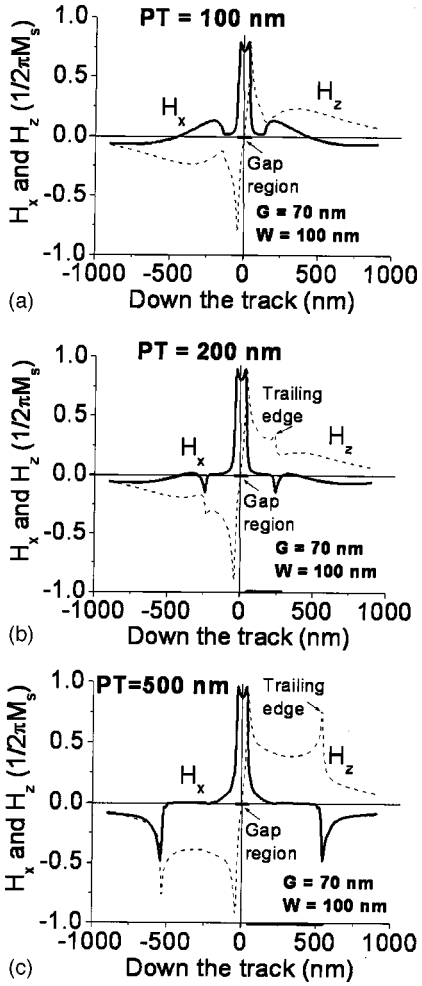

FIG. 6. Longitudinal and perpendicular field components vs the distance down the track for a RH with track width of 100 nm and gap length of 70 nm at three values of the pole thickness: (a) 100, (b) 200, and (c) 100 nm.

gap reaches $2\pi M_s$, the calculated saturated current versus the gap length is that shown in Fig. 5.

2. Trailing pole thickness dependence

The calculated field components for a gap length of 70 nm and a track width of 200 nm are shown for a set of three values of pole thickness, 100, 200, and 500 nm, in Figs. 6(a)–6(c), respectively. It can be noted that, although the longitudinal field component does not vary substantially as the pole thickness is increased from 100 to 500 nm, the perpendicular component increases by more than a factor of 3. Moreover, while the perpendicular component is noticeably smaller than the longitudinal component at the smallest value of the pole thickness, i.e., 100 nm, it becomes comparable to the longitudinal component as the pole thickness in increased to 500 nm.

In general, it could be noted that with respect to the recording field, the second perpendicular mode is quantitatively similar to the longitudinal mode. In both cases, the maximum field never exceeds $2\pi M_s$ of the head material. Previously, the implementation of the RH writer in combination with perpendicular media with a SUL has also been reported in the literature, therefore it is not going to be presented in this article.[22] In Sec. II B it is shown that the perpendicular recording field can be increased by at least a factor of 2, i.e., it can reach $4\pi M_s$, if a medium with a SUL is utilized.

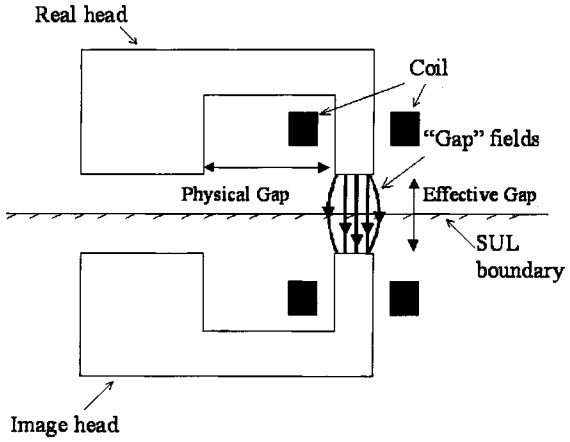

FIG. 7. Diagram showing a mirror image of a perpendicular system with an ideal soft underlayer.

B. First perpendicular mode: Single pole head and a perpendicular medium with a soft underlayer

As shown in Fig. 1(a), besides the presence of a SUL, the first mode is different from the second mode also in the type of recording head: it is a SPH instead of a RH. Unlike the RH, the SPH, utilized in combination with the SUL, has a physical gap that is substantially larger than the flying height. The purpose of the large gap is to force magnetic flux to flow through the SUL rather than through the gap region, thus enhancing the perpendicular component of the magnetic field. Therefore, the SUL is an indispensable part of the recording head as well as it is of the recording medium.

1. Magnetic image model

It is convenient to use the so-called ''magnetic image'' model for a clearer description of recording processes in a system with a SUL.[20] According to this model, the SUL is replaced with a half space, which contains a mirror image of the recording head, as shown in a schematic diagram in Fig. 7. This replacement is theoretically justified provided the SUL can be approximated to be ideal.[23] According to the theorem of differential equations, the Laplace equation (a consequence of the Maxwell equations, convenient to use for calculating the magnetic field) has an unambiguous solution if sufficient boundary conditions are satisfied.[24] It appears that in the case with the ideal SUL the boundary conditions at the SUL top surface are the same as those in the case with the mirror half space provided that the magnetic ''charges'' reverse their polarity when reflected into the mirror half space. Together with the image head, there are essentially two heads involved in each recording event, thus the net recording field becomes fairly large compared into the equivalent longitudinal case, as discussed below.

2. Permanent magnet approximation for SPH field calculations

The fastest way to estimate a magnetic field generated by a SPH at saturation is probably to use the permanent

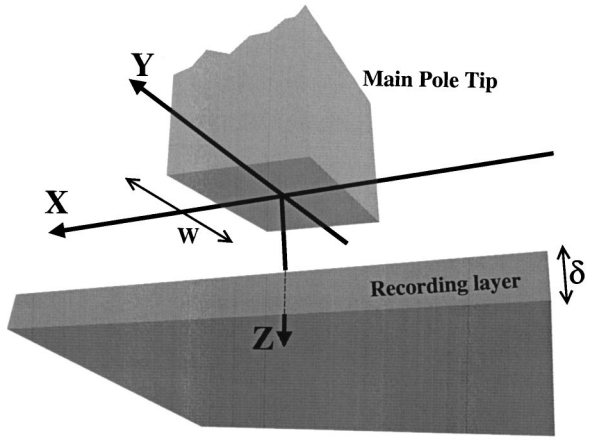

FIG. 8. Diagram showing the location of the origin of the coordinate system utilized in the calculations.

magnet approximation. In this approximation, the SPH is presented as an infinitely long vertical magnetic bar with finite cross-sectional dimensions, W (track width) and T (thickness), with its magnetization aligned (saturated) along the vertical axis. In this scenario, the magnetic field components can be directly calculated using, for example, the equivalent ''charge'' model.[25] Thus formulas derived for a saturated SPH without the presence of a soft underlayer are shown by expressions 1(a)–1(c). Because of the problem symmetry, it is sufficient to calculate the field in one coordinate quadrant, $x>0$ and $y>0$.

$$H_x=\frac{M_s}{2}\left\{\ln\left[\frac{y+\frac{b}{2}+\sqrt{\left(x-\frac{a}{2}\right)^2+\left(y+\frac{b}{2}\right)^2+z^2}}{y-\frac{b}{2}+\sqrt{\left(x-\frac{a}{2}\right)^2+\left(y-\frac{b}{2}\right)^2+z^2}}\right]-\ln\left[\frac{y+\frac{b}{2}+\sqrt{\left(x+\frac{a}{2}\right)^2+\left(y+\frac{b}{2}\right)^2+z^2}}{y-\frac{b}{2}-\sqrt{\left(x+\frac{a}{2}\right)^2+\left(y-\frac{b}{2}\right)^2+z^2}}\right]\right\}, \quad (1a)$$

$$H_y=\frac{M_s}{2}\left\{\ln\left[\frac{x+\frac{a}{2}+\sqrt{\left(x+\frac{a}{2}\right)^2+\left(y-\frac{b}{2}\right)^2+z^2}}{x-\frac{a}{2}-\sqrt{\left(x-\frac{a}{2}\right)^2+\left(y-\frac{b}{2}\right)^2+z^2}}\right]-\ln\left[\frac{x+\frac{a}{2}+\sqrt{\left(x+\frac{a}{2}\right)^2+\left(y+\frac{b}{2}\right)^2+z^2}}{x-\frac{a}{2}+\sqrt{\left(x-\frac{a}{2}\right)^2+\left(y+\frac{b}{2}\right)^2+z^2}}\right]\right\}, \quad (1b)$$

$$H_z=\frac{M_s}{4}\left\{\tan^{-1}\left[\frac{\left(x+\frac{a}{2}\right)\left(y+\frac{b}{2}\right)}{z\sqrt{\left(x+\frac{a}{2}\right)^2+\left(y+\frac{b}{2}\right)^2+z^2}}\right]-\tan^{-1}\left[\frac{\left(x-\frac{a}{2}\right)\left(y+\frac{b}{2}\right)}{z\sqrt{\left(x-\frac{a}{2}\right)^2+\left(y+\frac{b}{2}\right)^2+z^2}}\right]\right\}+\frac{M_s}{4}\left\{\tan^{-1}\left[\frac{\left(x-\frac{a}{2}\right)\left(y-\frac{b}{2}\right)}{z\sqrt{\left(x-\frac{a}{2}\right)^2+\left(y+\frac{b}{2}\right)^2+z^2}}\right]-\tan^{-1}\left[\frac{\left(x+\frac{a}{2}\right)\left(y-\frac{b}{2}\right)}{z\sqrt{\left(x+\frac{a}{2}\right)^2+\left(y-\frac{b}{2}\right)^2+z^2}}\right]\right\}. \quad (1c)$$

The origin of the coordinate system is at the center of the pole tip ABS with the vertical axis, Z, directed downward, as shown in Fig. 8. Moreover, the presence of the SUL can be simply taken into account by using the magnetic image model described above. In other words, the same expression can be utilized to calculate the extra recording field due to the image head located at the other side of the recording layer. The difference in spacing between the real and image heads is equal to the recording layer thickness plus the separation between the recording layer and the SUL. The sum of the two fields gives the total recording field.

3. Recording by the field in the gap (perpendicular) versus recording by the field fringing from the gap (longitudinal)

When using the magnetic mirror image model, besides the physical gap length, the effective (magnetic) gap length can also be introduced. The effective (magnetic) gap, defined as the spacing between the ABSs of the real and image heads, i.e., the twofold separation between the ABS and the SUL, can be meaningfully compared to the physical gap of the RH.[20] It can be noticed that the SPH considered along with its image resembles the RH rotated 90° around the axis along the cross-track direction, but with the difference that the recording is produced in the ''gap'' itself.[26] In contrast, in the longitudinal case as well as in the case of the second perpendicular mode, field fringing from the gap region produces the recording, as shown in Fig. 9. Any system that exploits a RH without a SUL is intrinsically built for the system to be efficient, so the gap length should be fairly small. It should be remembered that the more efficient a system is, the smaller the amount of magnetic flux that leaks out on its way from the source (drive coil) to its destination (ABS). Consequently, a substantial amount of magnetic flux

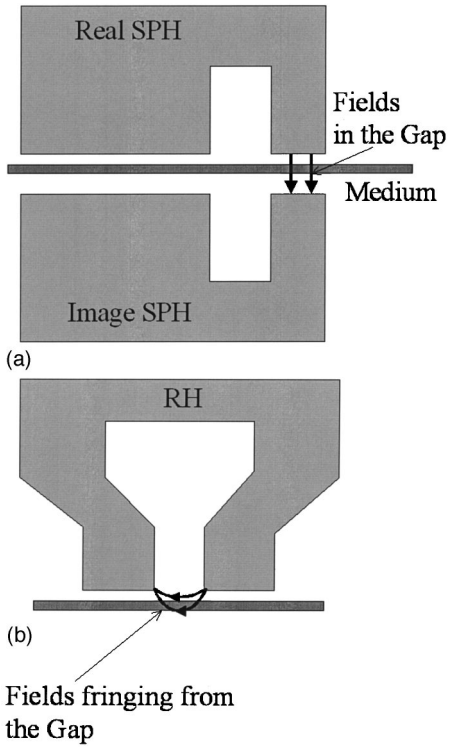

FIG. 9. Schematic diagrams showing (a) a recording by the field in the gap in perpendicular recording and (b) a recording by the fringing field in longitudinal recording.

just circulates in the magnetic ring yoke without being exploited for the purpose of recording itself, and, as noted above, only the fringing field produces the actual recording. Typically, the maximum fringing field which can be achieved in a recording system of this type is less than $2\pi M_s$, where M_s is the saturation magnetization of the head material.[21] This limits the coercivity of a longitudinal medium on which the recording head can record.[27] On the contrary, it is due to recording by the field in the gap region that the use of the SUL in the first perpendicular mode provides such a dramatic increase in the recording field at saturation. The calculated perpendicular and longitudinal field components for a SPH with a gap length, G, of 1000 nm, a pole thickness (PT) of 500 nm, and track width, W, of 100 nm at saturation are shown in Fig. 10. It can be noticed that in this case the maximum perpendicular field is of the order of $4\pi M_s$. This allows writing on a medium with a higher anisotropy field.

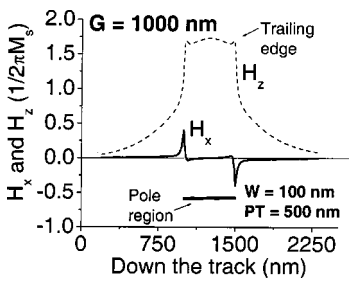

FIG. 10. Longitudinal and perpendicular field components vs the distance down the track (along the center line) for a SPH with gap length, G, of 1000 nm, pole thickness (PT) of 500 nm, and track width, W, of 100 nm.

The anisotropy field defines the field which needs to be applied to switch magnetization in the recording layer. In turn, the higher anisotropy medium means the higher density to which the superparamagnetic limit can be deferred. At this point, the SUL is assumed to be ideal. Also, the default modeling settings included a physical gap length of 1000 nm, a track width of 100 nm, and a throat height of 500 nm, with 20 nm separation between the ABS and the SUL. It can be noticed that, for the first perpendicular mode, the field profiles are qualitatively similar to the field profiles for the longitudinal mode shown in Fig. 4, provided that the field components are exchanged with each other according to the transformation $H_x \rightarrow H_y$ and $H_y \rightarrow -H_x$.[26] However, as previously mentioned, from a quantitative perspective, due to the use of the SUL the maximum perpendicular field in perpendicular recording is approximately a factor of 2 larger than the maximum longitudinal field in longitudinal recording.

4. Is the increase of the recording field due to the use of a SUL sufficient for proper recording?

The use of a soft underlayer provides a twofold increase of the recording field component compared to conventional longitudinal recording mode.[9] However, comparison of the two recording modes is not equivalent. Above, it was shown that, in the longitudinal mode, in the gap region, besides the longitudinal field component, there is also a substantial perpendicular component. For example, for a typical gap length of approximately 150 nm, as shown for the case in Fig. 4(c), both longitudinal and perpendicular components reach approximately the same value, i.e., $2\pi M_s$ of the head material. On the contrary, in the perpendicular mode, the maximum longitudinal field component is substantially less than the perpendicular field component. For example, for the case shown in Fig. 10, the perpendicular component almost reaches $4\pi M_s$, whereas the longitudinal component is substantially less than $1\pi M_s$, i.e., the difference is almost a factor of 4. As a result, the actual recording field is directed at angle values of approximately 45° and 15° with respect to medium magnetization for the longitudinal and perpendicular modes, respectively. From the ideal Stoner–Wohlfarth model, the switching field differs from the anisotropy field depending on the angle between the recording field and the easy axis.[28] Moreover, switching is expected to be substantially easier for the 45° case than 15° case. Another difference between these two recording modes results from the different nature of the recording medium. For the perpendicular case, the magnetization is aligned in one direction, i.e., the direction perpendicular to the disk plane, while, for the longitudinal case, the magnetization is directed randomly in the disk plane. Therefore, although realistic recording media might be substantially different from the ideal Stoner–Wohlfarth model, for a fair comparison of the two recording modes, all the factors described should be taken into account in more precise calculations. It is not done in this article because the purpose here is to describe the main concepts that help distinguish perpendicular recording. However, it can be noted that the second perpendicular mode, i.e., the mode without a soft underlayer, is based on the use of the

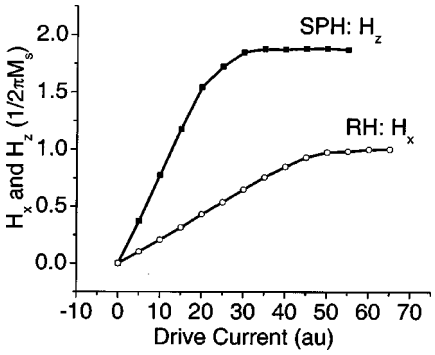

FIG. 11. Maximum recording fields for a RH and a SPH, each with track width of 500 nm, and a RH with throat height of 500 nm and gap length of 70 nm, and a SPH with a gap of 1000 nm, ABS to SUL separation of 35 nm, and throat height of 250 nm.

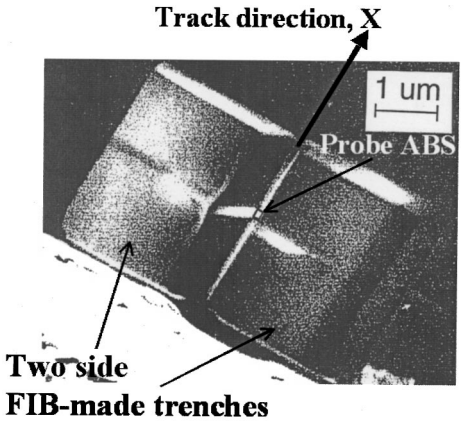

FIG. 12. SEM image of a FIB trimmed Censtor head (ABS view at 20° tilt).

ring type head, similar to the longitudinal mode, with all the advantages a result of the larger torque angle between the recording field and the magnetization. This similarity to the longitudinal mode makes implementation of the second mode simpler than implementation of the first mode. Therefore, the second mode should not be totally ignored.

5. Quadruple ratio between saturation currents in perpendicular and longitudinal recording

Another advantage of perpendicular recording which can be noted from the mirror image model is the fact that due to the SUL the effective number of current sources is essentially double (see Fig. 8). As a result, the perpendicular system needs approximately only half as much current to generate the same magnetic field in the effective gap compared to an equivalent longitudinal system. In Sec. II B6, it is shown that in the perpendicular case the recording is produced in the effective gap region. This is unlike the longitudinal mode, for which the recording is produced by field fringing from the gap. Because field fringing from the gap is about only one half the field in the gap and the effective number of drive current sources in the perpendicular system is twice that in the longitudinal system, for the perpendicular system it takes approximately four times less drive current to generate the same recording field as in the longitudinal system, with the other conditions equivalent. Although such a fairly rough estimate does not take into account any nonlinear effects that can take place in a recording system, it provides a good sense of the saturation currents in the two systems. As an example, the maximum recording fields generated by RH and SPH versus the drive current are shown in Fig. 11. In this calculation, each of the two heads was assumed to have the same track width of 500 nm. The RH was modeled with a gap length of 70 nm and a throat height of 500 nm, while the SPH was modeled with a pole thickness of 500 nm, a gap length of 1000 nm, an ABS to SUL separation of 35 nm, and a throat height of 250 nm. It can be noted that the linear region slope for the SPH is almost four times as large as the linear region slope for the RH. If recorded on media with the same coercivity, the saturation current for a perpendicular system should be four times less than it is for an equivalent longitudinal system.

6. Focused-ion-beam trimmed single pole heads

Using focused ion beam (FIB) trimming of regular relatively large RHs or/and SPHs, it is possible to fairly economically fabricate a set of individual recording SPHs with a required set of parameters, including the track width, pole thickness, gap length, throat height, shape of the leading (trailing) edge, and others.[29] Study of the FIB-fabricated devices can give good insight into the operation of realistic magnetic devices.

7. Example 1: FIB trimming of a wide-track Censtor SPH in a narrow-track SPH

Courtesy of Censtor Corporation, relatively wide SPHs (with approximately a 1 μm track width) were available for further modification via FIB trimming.[30] Modification included reduction of the track width down to approximately 100 nm. A scanning electron microscope (SEM) image of a FIB-fabricated 120 nm wide SPH is shown in Fig. 12.

MFM images of the perpendicular and longitudinal components of the field generated at the ABS of this head with drive current in the oversaturated regime (above 1000 mA turn) are shown in Figs. 13(a) and 13(b), respectively. The center cross sections of these field component profiles are shown in Fig. 13(c). Although there is no SUL in this case, the symmetry of the measured field profiles look similar to the symmetry of the modeled profiles with a SUL shown in Fig. 10. As mentioned above, the SUL has mostly a quantitative effect and thus does not substantially change the shape of the field profile.

8. Example 2: FIB trimming of a RH in a narrow-track SPH

Courtesy of IBM Corporation, relatively wide track RHs (with approximately a 1 μm track width) were available for further modification via FIB trimming. Modification included not only reduction of the track width down to approximately 60 nm, but also increase of the gap length from its original value of 150 nm to the required value of approximately 1 μm. A SEM image of the FIB-fabricated 60 nm wide SPH with 1 μm gap length is shown in Fig. 14.

A MFM image of two adjacent 65 nm wide tracks with periodic sets of transitions recorded onto a CoCr-based per-

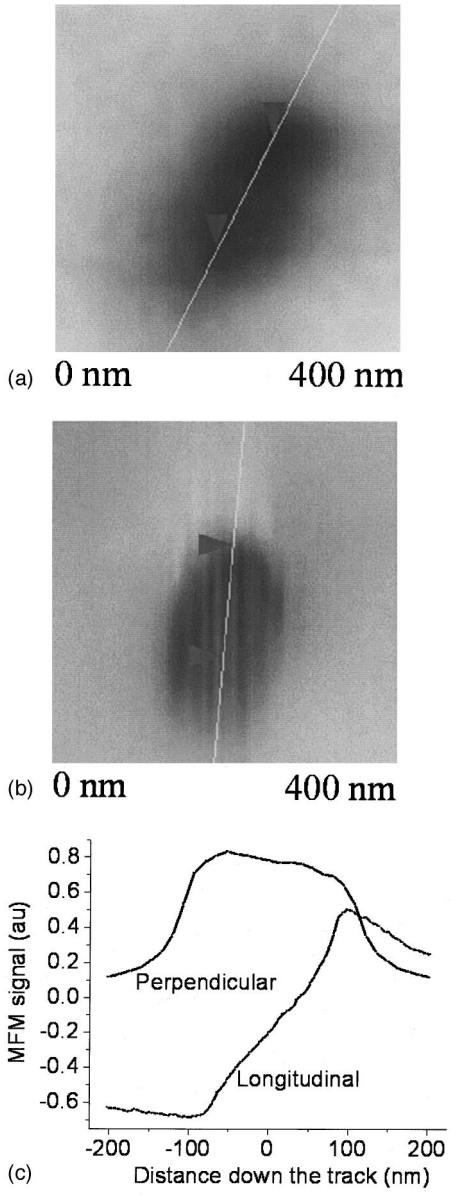

FIG. 13. MFM images of the (a) perpendicular and (b) longitudinal field components generated by a FIB trimmed Censtor head with track width of 120 nm and pole thickness of 200 nm. (c) Cross-sectional profile the perpendicular and longitudinal components.

pendicular medium with a SUL, shown in Fig. 15, clearly indicates the functionality of this fabricated SPH despite its nanoscale size track width. It should be remembered that there is a general concern that, as the SPH pole tip dimensions are reduced to sizes substantially less than the characteristic domain wall width in the soft material of which the pole tip is made up, the magnetization not only might become fairly ''hard'' to switch but also might display substantially nonzero remanence. A more detailed analysis of this is presented below.

9. Single pole head: Design strategy

A more detailed description of the SPH structure is now presented to explain the approach chosen to design the SPH geometry, shown in Fig. 16, and thus to clarify the limitations of this head design and motivate an approach for future modification. The limitations are fundamentally caused by the inability to infinitely maintain linear scaling of the system dimensions (to increase the areal density) below the value at which the flying height reaches the smallest value physically feasible. It is believed that it is unlikely to be able to maintain a steady flying height below approximately 5 nm because of its proximity to the size of the air molecules that critically participate in the recording head flying process. Therefore, deviation from straightforward scaling law is necessary to further increase the areal density. This can be accomplished by modification of the SPH design. Hence, understanding the principles utilized to design SPH geometry well make SPH modifications more efficient for satisfying the demand for an areal density increase.

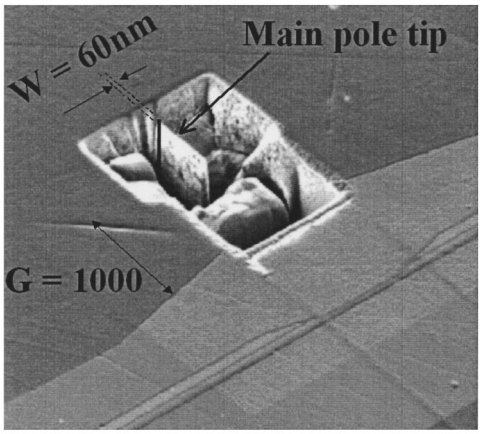

FIG. 14. SEM image of a SPH FIB made from a RH (ABS view at 40° tilt).

Before going into detail, it is worth mentioning the major requirements for a write head in perpendicular recording:

(1) the ability to generate a sufficiently strong field to record onto a medium with adequate coercivity;
(2) the ability to generate sufficiently large trailing and side field gradients to record sufficiently sharp transitions and narrow tracks, respectively;
(3) the ability to localize the recording field in a fairly limited region along the track so that the skew angle sensitivity is minimized (see Sec. II B13); and
(4) the ability to maintain reasonable efficiency of the recording system.

Below, analysis of the parameters which influence the above-listed requirements is presented. Before going into a description of the design methodology, it is worth mentioning that even today the flying height in every state-of-the-art

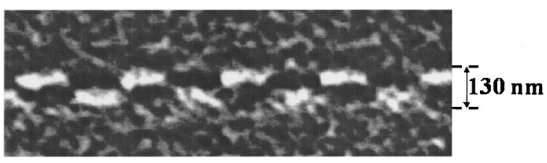

FIG. 15. MFM image of two adjacent 65 nm wide tracks recorded on a CoCr-based perpendicular medium with a SUL.

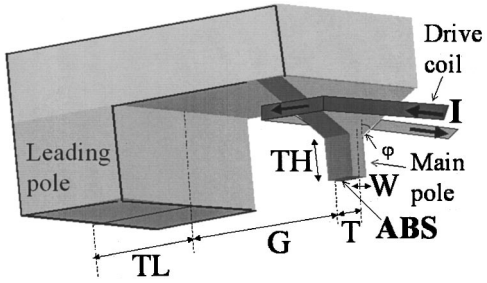

FIG. 16. Schematic diagram of a SPH.

recording system is of the order of 5 nm, which is already close to the size of the air molecule. Therefore, it is hard to see how the flying height can be further reduced, because the air flow process is a critical link in ultimate operation of a magnetic hard drive. This means that the established over decades trend of increasing the recording density in a magnetic recording system only by direct application of the scaling law should be adjusted to create next generation magnetic technologies. In other words, to obtain the maximum benefit and achieve the highest possible areal density, special attention should be given to each component of the magnetic recording system.

10. Definition of efficiency

Before going into details of the design, a basic quality indicator such as the efficiency of a recording system should be redefined for perpendicular recording.[11] In longitudinal recording, the efficiency is the ratio of the magnetic flux generated in the deep gap of the RH and the flux in the drive coil.[19] As mentioned above, for perpendicular recording it is not the physical gap but rather the effective (magnetic) gap, defined as the separation between the SPH and its image, that is equivalent to the physical gap of the RH. Therefore, it makes sense to define the efficiency, η, of a magnetic system of the first perpendicular mode as the ratio of the magnetic flux in the magnetic gap (the flux under the pole tip ABS) and the flux in the drive coil, as shown in Fig. 17,

$$\eta = B_{\mathrm{gap}} A_{\mathrm{gap}} / NI,$$

where A_{gap} is the deep gap cross-sectional area.

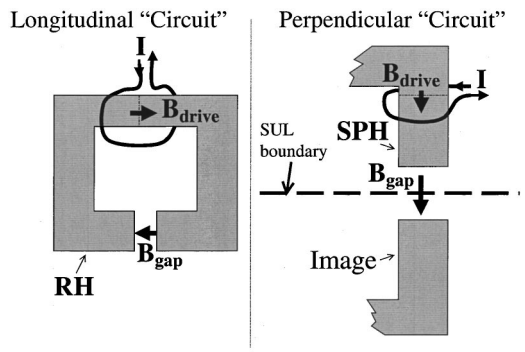

FIG. 17. Diagrams showing magnetic ''circuits'' in a longitudinal system with a RH and a perpendicular system with a SPH and a SUL.

11. Throat height dependence

The throat, being the narrowest part of the magnetic flux loop (circuit), typically is also the highest reluctance link of the magnetic loop.[31] Thus, by reducing the throat height, the relative contribution of the throat region to the net reluctance of the magnetic circuit is also reduced and therefore the overall efficiency of the system is increased. Also, as described below, by reducing the throat height, the recording field at saturation is increased. There are two competing factors that contribute to the increase in recording field as a result of throat height reduction. First, the field is increased because, as a result of throat height reduction, the point inside the pole tip at which saturation starts to occur is shifted closer to the ABS. Calculated magnetization contours along the center cross-track planes inside the main pole tip in two extreme cases with fairly tall sufficiently short throats are shown in Figs. 18(a) and 18(b), respectively. The magnetization profiles at saturation along the center vertical line inside the pole tip for these two cases are shown in Fig. 18(c). It can be observed that, for the tall throat, saturation occurs near the top region of the throat, thus only a relatively small part of the initial magnetic flux generated by the drive coil reaches the ABS. As the current is increased beyond the saturation value, most of the flux is going to leak out of the magnetic loop on its way from the drive coil to the ABS. In contrast, for the short throat, saturation starts to take place at the ABS, thus the maximum possible flux reaches the ABS and therefore the maximum possible field (for a flat surface, of the order of $4\pi M_s$) can be generated. In other words, in the latter case, there is essentially more magnetic charge generated at the ABS. The charge at the ABS is the source required for the recording field.

Because charge is located at the ABS, the ABS dimensions of the pole tip determine the recorded bit size. Therefore, being local in origin, this is a favorable effect of throat height reduction. Unfortunately, the throat height reduction results in another effect which deteriorates the field gradients. This effect is due to charges created on the tilted walls above the throat height of the main pole, as shown in Fig. 19. These charges generate an extra field which is not localized and therefore results in deterioration of the field gradients, as shown below. As the throat height is reduced, the charge at tilted walls moves closer to the ABS, and thus, the contribution of this unfavorable field increases.

It should be remembered that, although a perpendicular medium is ideally symmetric with respect to any of the two in-plane directions, i.e., along and across the track, a typical SPH, shown in Fig. 19, is not.[32] Because of fabrication process limitations, typically the throat top boundaries (the lines at which walls start to deviate from being vertical) are defined only at the two cross-track side walls of the main pole, and not at any of the two along-track side walls, as shown in Fig. 19. It should be noted that magnetic charge is proportional to the change in magnetization component normal to the boundary surface.[33] Therefore, in this particular case, the magnetic charge is concentrated on the cross-track sides rather than on the leading and trailing sides of the main pole. As a result, because of the different amount of the charge in these two cases, the throat height dependence might be quan-

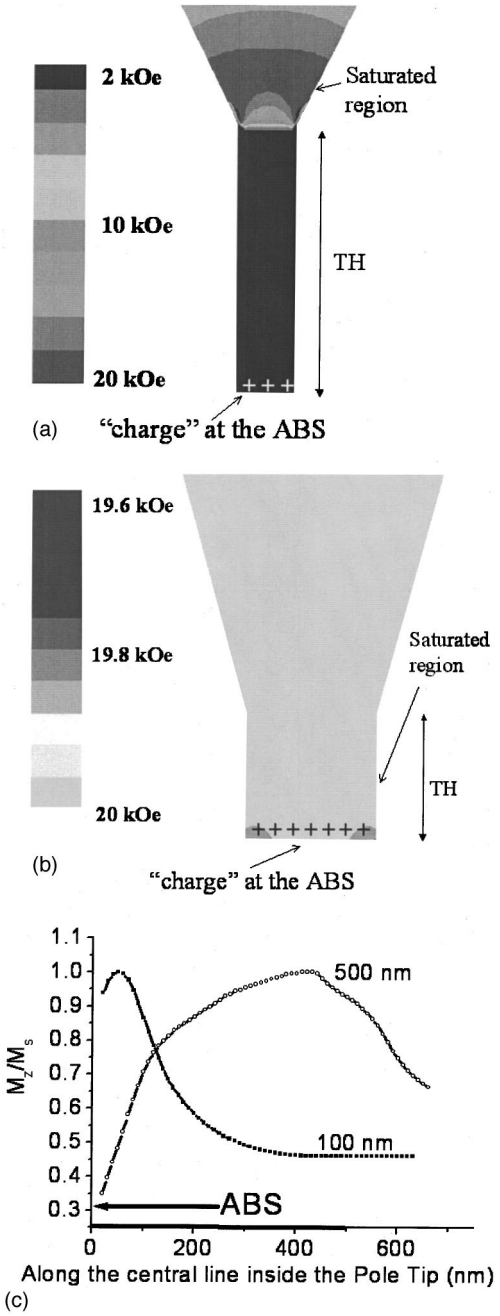

FIG. 18. Calculated magnetization contours along the center cross-track planes inside the main pole for two extreme cases at saturation: (a) a fairly tall throat and (b) a sufficiently short throat. (c) Magnetization profiles along the center vertical line for the two cases at saturation.

titatively different for field profiles along and across the track, respectively, as shown below.

The along-track profiles of the perpendicular field component and its normalized value at 5 nm flying height and 20 nm separation between the ABS and the SUL at different values of drive current (in arbitrary units) for two values of throat height, 100 and 500 nm, are shown in Figs. 20(a) and 20(b), respectively. In this case, the sidewall tilt angle, φ, shown in Fig. 19, was modeled to be 45°. The perpendicular fields and their normalized values for the same set of parameters across the track are shown in Figs. 21(a) and 21(b), respectively. As expected, it is observed that, although it is

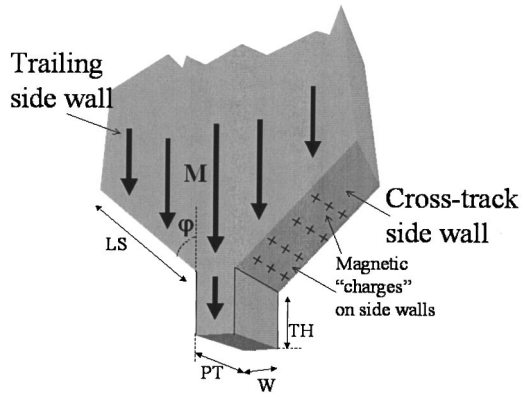

FIG. 19. Diagram of a SPH pole tip showing the location of sidewall charges.

easier to drive more recording field in the case of the shorter throat, the undesirable off-track side field also increases due to an increase in charge at the tilted sidewalls. To illustrate this effect, two cross-track perpendicular field profiles that correspond to the two throat height values at saturation are shown in Fig. 22(a). The same profiles normalized to corresponding values at the center of the track are shown in Fig. 22(b). The normalized profiles directly illustrate the fact that the shape of the field profile is substantially wider in the shorter throat height case.

The field 5 nm below the center of the main pole versus the drive current at three values of throat height, 100, 200, and 500 nm, is shown in Fig. 23(a). The drive current is given in arbitrary units because the exact value of the current depends on a number specific to each head design parameter, such as the exact location of the drive coil with respect to the ABS, the yoke geometry, etc. The saturation current can be defined at the value at which the first discontinuity (change of slope) in field dependence on the current takes place. This

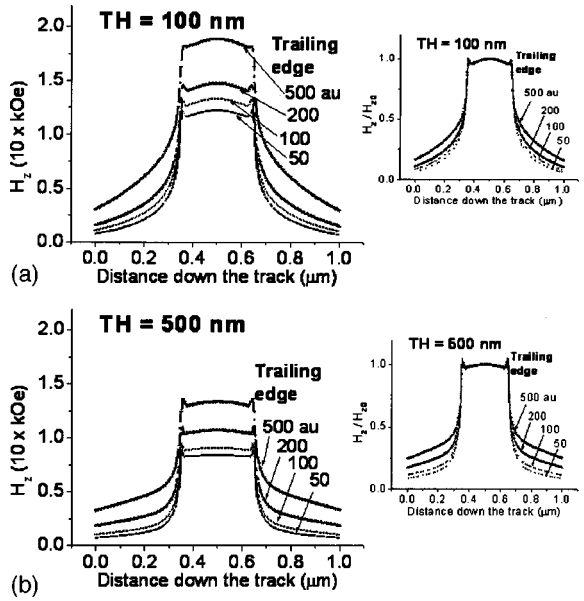

FIG. 20. Along-track profiles of the perpendicular field component and its normalized value for two values of the throat height: (a) 100 and (b) 500 nm.

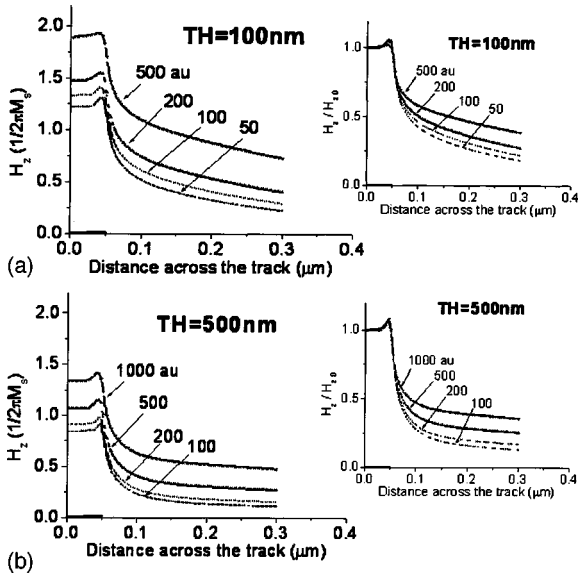

FIG. 21. Cross-track profiles of the perpendicular field component and its normalized value for two values of the throat height: (a) 100 and (b) 500 nm.

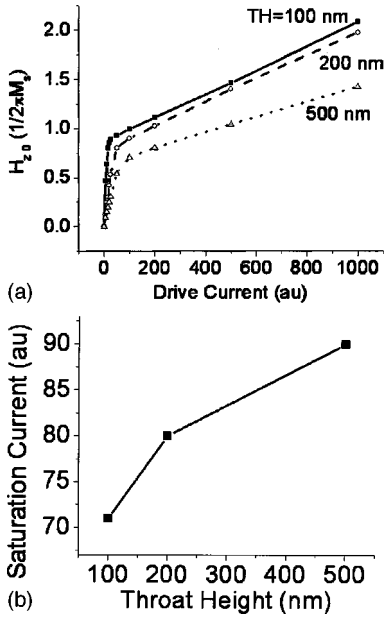

FIG. 23. (a) Perpendicular field vs the drive current at three values of the throat height: 100, 200, and 500 nm. (b) Saturation current vs the throat height.

derived saturation current (reflecting system efficiency) versus the throat height is shown in Fig. 23(b). In summary, reduction of the throat height has two favorable effects, an increase of the recording field and reduction of the saturation current. However, the throat height cannot be reduced entirely to zero, because the smaller the throat height, the poorer the side and trailing field gradients, as noted above (see Fig. 22).

Here, it should be mentioned that, for an ideally saturated state, the field due to side charge can be easily calculated according to the Coulomb law for the "magnetic" charges on the sidewalls. It can be shown that at zero throat height and tilt angle of 45° the extra field due to the side charges can substantially overcome $4\pi M_s$ (the maximum field assuming a pole tip with no charge in sidewall) provided the sidewall is sufficiently tall. Considering the side nature of the source of this field, the field due to the side charge not only increases the field under the pole tip (on the track) but also creates an unfavorable field at the sides (off the track) and thus deteriorates the field gradient. Therefore, to minimize the contribution of side charge, it is preferable to keep a sufficiently tall throat. In other words, there is a trade-off between the field magnitude and the field gradient, and this trade-off can be controlled by the throat height.

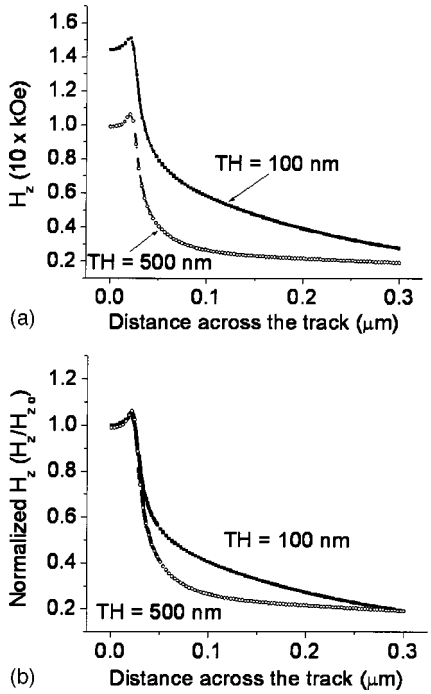

FIG. 22. (a) Cross-track profiles at saturation for two values of the throat height: 100 and 500 nm. (b) Normalized profiles at saturation.

12. Dependence on the pole track width and thickness

Another way to increase the recording field is to make each ABS cross-sectional dimension of the SPH pole tip (pole thickness and track width) as large as possible.[34] The characteristic dimension at which the field starts to substantially change is determined by double the (due the "image" by the SUL) distance between the ABS and the SUL. The track width, W, of the SPH determines how narrow a track can be recorded. Therefore, the track width value is set by a required areal density value. For example, at an areal density beyond 100 Gbit/in.^{2}, the track pitch (the track width plus the guard band) should be smaller than approximately 160 nm, assuming a 4:1 bit aspect ratio (BAR). Assuming that the guard band occupies approximately one fifth (20%) of the track pitch, the SPH should have a track width of approximately 120 nm to record an approximately 130 nm wide track. As for the pole thickness, as previously mentioned, in perpendicular recording, ideally the actual recording takes place only near the trailing edge of the pole, therefore, one can have pole thickness as large as necessary for a maximum

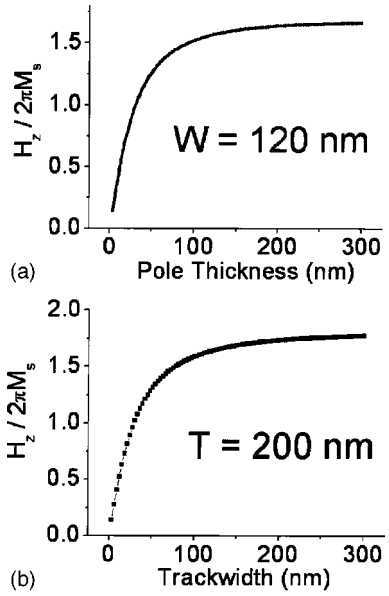

FIG. 24. Maximum field at saturation vs (a) the pole thickness for a SPH with track width of 200 nm and (b) the pole track width at a fixed value of the thickness, 200 nm.

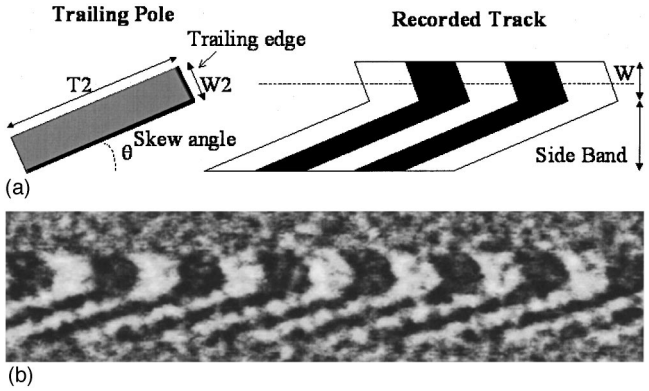

FIG. 25. (a) Diagram showing the ABS of a pole with skew with respect to the track direction and transitions recorded with the skewed trailing pole, thus creating a recorded track. (b) MFM image of a track recorded by a SPH head on a CoCr-based perpendicular medium at 15° skew angle.

increase of the recording field. The maximum recording at saturation versus the pole thickness for a given track width of 120 nm is shown in Fig. 24(a). However, in practice, as explained below, the pole thickness cannot be made infinitely long because, in a real hard drive, the skew angle is not always zero. The nonzero skew angle results in effectively recording a substantially wider track compared to the track width of the pole tip. As shown below, the pole thickness value of approximately 200 nm should reduce the skew angle sensitivity to few percent of the track width value, assuming an approximately 10° maximum skew angle and areal densities below approximately 400 Gbit/in.^{2} At 400 Gbit/in.^{2} areal density, assuming a 4:1 bit aspect ratio, the recorded track pitch should be 80 nm wide. Therefore, the track width of the pole tip should be smaller than 80 nm. The maximum saturation field versus the pole track width at a fixed value of pole thickness of 200 nm is shown in Fig. 24(b). At this point, it is worth noting that the image head is located further away from the center of the recording layer than the real head, as shown in Fig. 9, with the difference in spacing equal to the recording layer thickness. Ideally, the net recording field of $4\pi M_s$ can be produced as a result of contributions by fields generated by both the real and image heads, respectively, with a $2\pi M_s$ field per each head. Assuming 30 nm separation between the ABS and the SUL, at such high areal densities the track width ($\sim<80$ nm) is of the same order of magnitude as double the separation between the ABS and the SUL. Therefore, it is not unnatural that the net recording field starts to substantially drop as the track width is further reduced.

In summary, ideally, assuming a zero skew angle, the pole thickness can be made infinitely large because the recording is produced only near the trailing edge. Nevertheless, the increase in thickness results only in an approximately 30% increase if the track width is kept as small as 120 nm. Moreover, in real conditions with nonzero skew, the nonzero length of the pole thickness, T, results in substantial side recording, as explained next.

13. Skew angle sensitivity of single pole head

One of the most serious issues in future implementation of perpendicular recording is believed to be the excessive sensitivity of a typical perpendicular recording system to the skew angle.[8,35] As mentioned above, unlike in longitudinal recording, for which the recording is produced by the fringing field in the physical gap region of a RH, shown in Fig. 2, in perpendicular recording, the recording is produced in the gap near the trailing edge of the main pole of a SPH, shown in Fig. 1. As a result, one of the principal differences is the order of magnitude difference between typical sizes of the gap region of the RH and the trailing pole thickness of the SPH. For state-of-the-art recording RH and SPH suitable for areal densities of the order of 100 Gbit/in.^{2}, for example, the gap thickness and the trailing pole thickness are of the order of 50 and 1000 nm, respectively. This substantially larger thickness of the SPH pole results in it being extremely sensitive to the skew angle. To help in understanding this, a diagram of a track recorded by a SPH at nonzero skew angle is shown in Fig. 25(a). It can be noted that at the condition of nonzero skew angle the recording is produced not only by the trailing edge but also by one of the sides of the trailing pole. A MFM image of a real track recorded with a SPH with a 500 nm thick pole at 15° skew angle on a CoCr-based perpendicular medium is shown in Fig. 25(b).

It is clear, therefore, that the thicker the trailing pole is, the more sensitive the system is to the skew angle. To a sufficient degree of approximation, the side written region is proportional to the product of $T2 \times \sin\theta$, where $T2$ and θ are the pole thickness and the skew angle, respectively, as shown in Fig. 26. Assuming typical values for $T2$ and θ of approximately 1000 nm and 10°, respectively, the side written region can be of the order of 150 nm, which is unacceptable at areal densities beyond 100 Gbit/in.^{2} It should be remembered that the entire track width is expected to be less than 150 nm at such high densities assuming a 4:1 BAR.

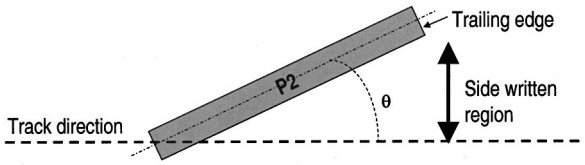

FIG. 26. Diagram showing how the side recording is generated due to a nonzero skew angle.

The most straightforward ''solution'' for eliminating the skew sensitivity is reduction of the pole thickness. However, this solution is not adequate, because in this case the recording field drops drastically and thus recording on a sufficiently high coercivity medium becomes problematic.[27] As an example, the calculated perpendicular field at saturation versus the distance down the track near the trailing pole edge with 120 nm track width and 20 nm separation between the ABS and the SUL at two different values of pole thickness, 100 and 500 nm, is shown in Fig. 27. In this calculation, the SPH and SUL were modeled to be made of a relatively high moment material with $4\pi M_s$ of 2 T.[36] It can be seen that reduction of the pole thickness to 100 nm reduces the field by almost a factor of 2. Another approach needs to be found to solve the fundamental issue of skew angle sensitivity. It was shown that the use of a trapezoidal write pole can partially reduce the skew sensitivity.[37,38] Good understanding of the mechanisms that determine the recording field will help in finding a more drastic solution.

14. Gap length dependence

In Sec. II A, it was shown that as a direct consequence of recording by field fringing from the gap, properties of a system that utilize a RH without a SUL, regardless of whether it is perpendicular or longitudinal recording, fairly strongly depend on the physical gap length, as discussed above. This is in contrast with the case of the first perpendicular mode, for which no significant dependence on the physical gap length can be expected as long as the gap length is substantially larger than the separation between the ABS and the SUL. For the second perpendicular mode, the physical gap is part of the main path for magnetic flux in a recording system. As a result, in case of the second mode, stronger dependence on the gap length is expected. On the contrary, for the first perpendicular mode, the main path for magnetic flux does not go through the physical gap region, rather it goes through the SUL, which explains the substantially weaker dependence on the physical gap length as long as the gap is substantially larger than the separation between the ABS and the SUL. Detailed analysis of the physical gap's influence on the recording characteristic of a system with a SUL can be found elsewhere.[22]

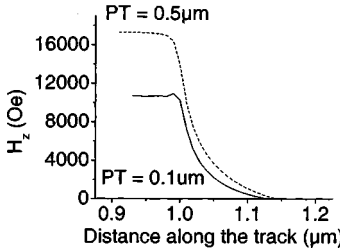

FIG. 27. Modeled vertical fields near the trailing edge for two values of the pole thickness, PT: 0.5 and 0.1 μm, with the same track width of 0.1 μm.

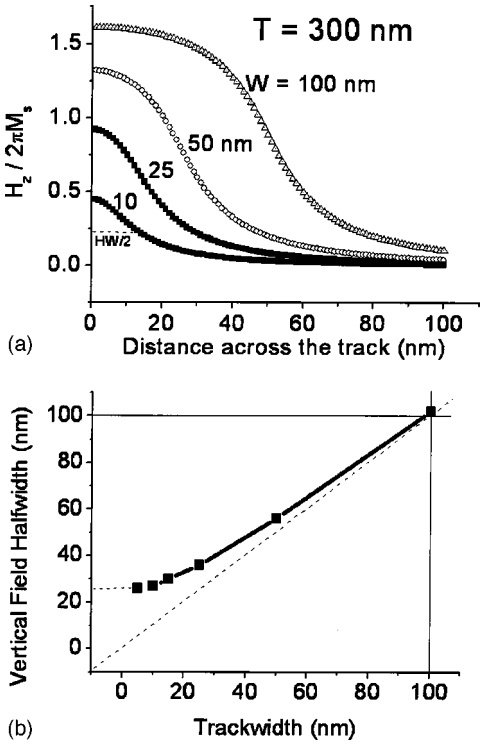

FIG. 28. (a) Vertical field vs the distance across the track at saturation for a SPH with 300 nm thickness at three values of the track width: 25, 50, and 100 nm. (b) Field half width vs the track width.

15. Flying height limitation of a single pole head design

As mentioned above, the fundamental density limitation of the regular SPH design is due to the inability to scale the flying height as areal density increase demands reduction of the flying height to values below physically impossible.[27] For example, it is believed that the smallest achievable flying height is approximately 5 nm. It is hard to see how one can make the flying height smaller considering that 5 nm is already of the order of the size of the air molecule. Therefore, assuming a constant flying height of approximately 5 nm, as the track width is reduced to satisfy the areal density increase, the field generated at the recording layer also decreases. Unfortunately, the field magnitude cannot be endlessly maintained via reduction of the throat height. As shown above, as the throat height becomes too small, the contribution to the recording field from magnetic charge on the tilted sidewalls increases. As a result, the cross-track and trailing field gradients deteriorate.[21] Assuming the sidewall tilt angle is approximately 45°, the smallest value of throat height at which gradient deterioration is less than 50% is approximately 100 nm. The recording field generated at saturation under the center of a 300 nm thick trailing pole with 100 nm throat height at 5 nm flying height versus the distance across the track at three values of track width, 25, 50, and 100 nm, is shown in Fig. 28(a). For example, at 1

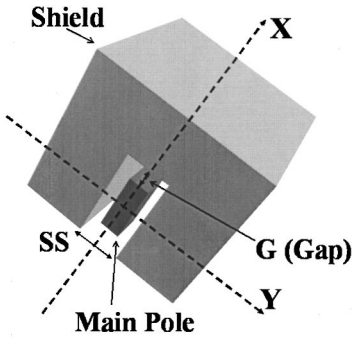

FIG. 29. Diagram of the ABS of a shielded single pole head pole tip configuration.

Tbit/in.^{2} density, the track width is approximately 50 nm assuming a 4:1 BAR. The signal half width defined as the distance along the track at which the signal drops twice from its maximum value versus the track width is shown in Fig. 28(b). It can be noted that, as the track width becomes narrower than approximately 50 nm, the half width ceases to strongly depend on the track width. This is explained by the fact that, as the track width is reduced below this critical value, the half width is predominantly determined by the doubled separation between the ABS and the SUL along with the flying height, which, in this case, is 20 and 5 nm, respectively. Also, as the track width is reduced below approximately 50 nm, the field magnitude drastically decreases for two reasons: (1) the field generated by an individual SPH drops as the track width is reduced because the net magnetic charge is reduced and (2) the contribution by the field generated by the image SPH drops faster with a reduction in track width because it is essentially further away from the center of the recording layer compared to the real SPH.

In summary, the main question regarding the write head at areal densities of the order of 1 Tbit/in.^{2} can be formulated as follows: How can one maintain the recording field magnitude with reduction of the bit dimensions without deteriorating the field gradients?

C. Modified first perpendicular mode: Shielded single pole head and a perpendicular medium with a soft underlayer

1. Shielded single pole head

One of the previously proposed solutions is to build soft magnetic shields around the main pole, as shown in Fig. 29.[39]

It can be noted that the shields are wrapped only around the trailing side and the two cross-track sides of the main pole. Only these three sides are critical for recording, because the two cross-track sides define the track width and the trailing side defines the quality of each linear transition. No recording is supposed to take place at the leading side, therefore, this side does not necessarily have to be covered with a shield. The direct effect of shielding is screening the unfavorable side field from the recording medium, as shown in a cross-track cross-sectional diagram in Fig. 30. Consequently, the constraints on the head structure, which were placed on the regular SPH (without shielding) to reduce the effect of

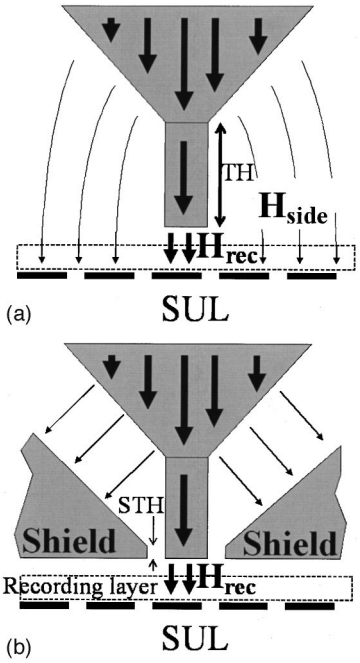

FIG. 30. Diagrams showing propagation of the magnetic field for the two cases of interest: (a) those without and (b) those with shields.

the side field, are substantially relaxed if shields are utilized. It should be remembered that, for the regular SPH, the pole tip geometry is chosen with a fairly large throat height to reduce the side field. The cost of the fairly tall throat is substantial reduction of the field magnitude and system efficiency, as shown above. On the contrary, for the case with shields, the throat height can be substantially reduced to maintain fairly large field magnitude without losing field gradients. In other words, if shields are used, a substantially more efficient pole structure can be implemented without losing the field gradient. As an example, calculations were made to compare the recording field generated by a regular SPH with throat height (TH) of 100 nm with the recording field generated by a shielded SPH (SSPH) with 50 nm throat height and cross-track shield to shield separation of 90 nm and downtrack gap, *G*, between the write pole and the trailing shield of 20 nm. The shield throat height (STH) was modeled to be 10 nm. In both cases, the pole tip was modeled to be 50 nm wide and 300 nm thick. The center cross-track profiles for these two cases at saturation are shown in Fig. 31. In practice, however, there might be limitations due

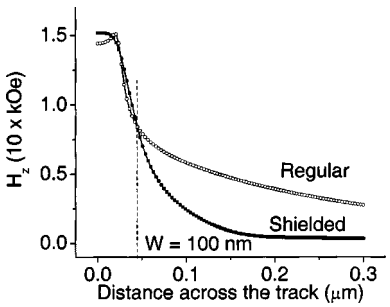

FIG. 31. Cross-track profiles for a regular SPH and a shielded SPH at saturation.

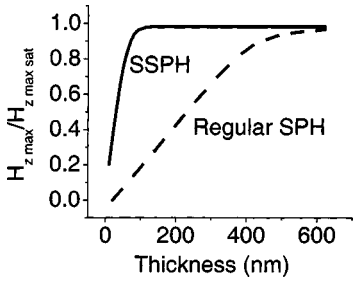

FIG. 32. Maximum trailing field at saturation (normalized to its saturation value) vs the pole tip thickness for a regular SPH with 500 nm throat height and a shielded SPH with zero throat height. The track width is 120 nm.

to difficulties in processing. For example, the shortest possible today throat height is going to be dictated by the lapping process accuracy.

As a direct consequence of the ability to exploit a more efficient pole tip configuration, the improved skew angle performance of the SSPH should be mentioned. Due to higher efficiency than SPH, a much thinner pole tip can be utilized to generate the same recording field. Therefore, the SSPH has substantially improved skew angle performance compared to SPH, as discussed below.

For design of the SSPH, the side cross-track and trailing field gradients are predominantly determined by the spacing between the main pole and the shields. This is in contrast to the regular nonshielded SPH design, for which the gradients are determined not only by the flying height and the separation between the ABS and the SUL but also to significant degree by the throat height. Evidently, the deadly limitation of a nonzero throat height in the case of the regular SPH design is automatically removed in the case of the SSPH design. In the latter case, even for a substantially shorter throat height, the undesired side cross-track and trailing fields are reduced due to the existence of a relatively low-reluctance well-defined return flux path via the shields.

As noted above, the reduction of throat height to zero dramatically increases the system efficiency and allows a substantially larger amount of magnetic flux generated by the drive coil to reach the ABS. This automatically results in better skew angle performance of the SSPH design compared to the conventional SPH design, because in this case a head with a substantially thinner pole tip can be utilized to generate a field as strong as the field generated by an equivalent conventional SPH with a much thicker main pole tip. As discussed above, the skew angle sensitivity is proportional to the pole tip thickness. The maximum trailing field at saturation versus the main pole thickness for the two cases, a regular SPH with 500 nm throat height and SSPH with zero throat height, both with 120 nm track width, is shown in Fig. 32. To clearly illustrate the point, the field is shown normalized to its saturation value. It can be noted that the field does indeed start to drop at a smaller thickness for the case with shields.

Another observation that can be made is the fact that if shields around the main pole are utilized, as described above, there is absolutely no need for the return pole to be separated by a fairly large gap from the leading edge of the main pole,

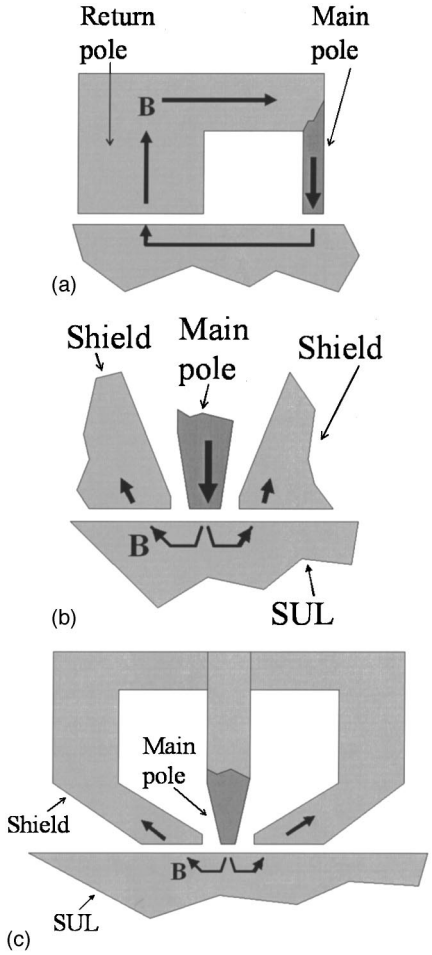

FIG. 33. Diagrams showing the flux return paths for (a) a regular SPH (along-track cross-sectional view) and (b) a shielded SPH (front view cross section), respectively. (c) Full-scale front view cross section of the SSPH.

as shown in Fig. 33. The shields wrapped around the main pole not only act as gradient shapers but also play the role of return pole. As a result, a system with shields around the main pole and without a return pole remains approximately as efficient as a regular system with a return pole.

As a consequence of the shields acting also as a flux return pole, the requirements for use of a SUL are much less tight than in the regular SPH case. It can be also observed that the shielded structure resembles a typical ring head structure. The purpose of the separation between shields and the main pole is to avoid the side field and thus to distinctly define recording transitions. Similarly, the purpose of the gap between the two poles of the ring head structure is to define recording transitions. Moreover, similar to a system with a ring head, a system that utilizes a shielded writer can be utilized without any SUL at all. As shown in Fig. 33(b), the fairly small separation between the main pole and the shield provides sufficient efficiency. In most implementations, shields are coupled to the main pole through the back of the pole, as shown in Fig. 33(c). In this case, the trailing and cross-track side field gradients are determined by the flying height and the separation between the main pole and the shields rather than by the separation between the ABS and the SUL. As a matter of fact, for the dimensions considered, the only noticeable difference between the two modified sys-

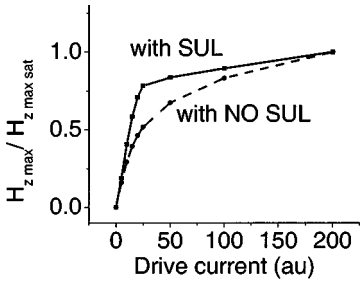

FIG. 34. Maximum field vs the drive current for two configurations: a SSPH with and without a SUL. The field is shown normalized to its saturation value.

tems, that with and that without a SUL, is the fact that the systems without a SUL need approximately 20% more current to saturate, as shown in the calculated current dependences in Fig. 34. To clearly illustrate the main dependence, the field is shown normalized to its saturation value.

In summary, it can be concluded that the utilization of soft magnetic shields around the main pole results in the following advantages.

(1) The recording field can be maintained fairly large without field gradient degradation at higher areal densities, compared to the case without shields.
(2) The field gradient can be controlled by varying the separation between the main pole and the shields as well as by the pole tip and shield geometry.
(3) If shields are used, the system efficiency can be increased by the substantial reduction of the throat height. As a consequence, the skew angle sensitivity can be substantially reduced.

III. CONCLUSIONS

In this article, a detailed overview of the methodology to design a write transducer for recording on perpendicular media at areal densities beyond 1 Tbit/in.^{2} was presented. The two basic modes of perpendicular recording, single-layer recording media in combination with a ring type head and double-layer recording media with a soft underlayer in combination with a single pole head, were compared with each other theoretically and experimentally. It was shown that in the latter case, due to the use of the SUL, the recording field can be increased by approximately a factor of 2. However, it is also shown that the price for the increase of recording field can be substantial degradation in the trailing field gradient unless a thorough analysis is made to choose an adequate design. Moreover, perpendicular recording was compared to longitudinal recording from the perspective of the writing process. The system efficiency was redefined for perpendicular recording to take into account the critical role of the soft underlayer. It was shown that a system in the perpendicular mode with a SUL needs less current for saturation, compared to an equivalent system in the longitudinal mode. The effects of using ''soft'' magnetic shields around the trailing pole were analyzed. It was shown that at least a factor of 2 increase in field can be obtained at areal densities beyond 500 Gbit/in. if shields are used. This unresolved issue of skew angle sensitivity in perpendicular recording was analyzed. It was shown that using soft magnetic shields around the trailing pole substantially improves the skew angle sensitivity. Moreover, using shields substantially improves the system efficiency and to some degree fulfills the role of the soft underlayer in perpendicular recording.

[1] S. H. Charap, P.-L. Lu, and Y. He, IEEE Trans. Magn. **33**, 978 (1997).
[2] Materials Research Society Bulletin, May 2003, p. 387.
[3] S. Iwasaki, IEEE Trans. Magn. **39**, 1868 (2003).
[4] A. S. Hoagland, IEEE Trans. Magn. **39**, 1871 (2003).
[5] F. Liu *et al.*, IEEE Trans. Magn. **39**, 1942 (2003).
[6] Private communications with Mark Kryder, CTO, Seagate Technology (2003).
[7] S. Iwasaki and Y. Nakamura, IEEE Trans. Magn. **13**, 1272 (1977).
[8] D. A. Thompson, J. Phys. Soc. Jpn. **21**, 9 (1997).
[9] S. Khizroev, M. Kryder, and D. Litvinov, IEEE Trans. Magn. **37**, 1922 (2001).
[10] D. Litvinov, M. Kryder, and S. Khizroev, J. Magn. Magn. Mater. **232**, 84 (2001).
[11] *Magnetic Recording*, Volume III: Video, Audio, and Instrumentation Recording, edited by C. D. Mee and E. D. Daniel (McGraw–Hill, New York, 1988).
[12] M. H. Kryder, W. Messner, and L. R. Carley, J. Appl. Phys. **79**, 4485 (1996).
[13] D. Litvinov, M. Kryder, and S. Khizroev, J. Magn. Magn. Mater. **241**, 453 (2002).
[14] M. L. Williams and R. L. Comstock, 17th Annual Conference Proceedings, Part 1, No. 5 (2002), pp. 738–742.
[15] See www.readrite.com.
[16] D. Litvinov and S. Khizroev, Appl. Phys. Lett. **81**, 1878 (2002); Virtual J. Nanoscale Sci. Technol., September 9th (2002).
[17] O. Karlqvist, Trans. R. Inst. Technol. Stockholm **86**, 3 (1954).
[18] Amperes, Integrated Inc., Canada.
[19] R. E. Jones, Jr., IEEE Trans. Magn. **14**, 509 (1978).
[20] S. Khizroev, Y. Liu, K. Mountfield, M. Kryder, and D. Litvinov, J. Magn. Magn. Mater. **246**, 335 (2002).
[21] M. H. Kryder and W.-Y. Lai, IEEE Trans. Magn. **30**, 3873 (1994).
[22] D. Litvinov, J. Wolfson, J. A. Bain, R. W. Gustafson, M. H. Kryder, and S. Khizroev, IEEE Trans. Magn. **38**, 2252 (2002).
[23] D. Litvinov, R. Chomko, G. Chen, L. Abelmann, K. Ramstock, and S. Khizroev, IEEE Trans. Magn. **36**, 2483 (2001).
[24] M. V. Fedoryuk *et al.*, ''Asymptotic analysis: linear ordinary differential equations,'' Berlin, Springer, 1993.
[25] Soshin Chikazumi, Physics of Ferromagnetism, 2nd Edition, Oxford University Press, 1997.
[26] S. Khizroev and D. Litvinov, J. Magn. Magn. Mater. **257**, 126 (2003).
[27] M. H. Kryder, Sci. Am. **117**, 72 (1987).
[28] E. C. Stoner and E. P. Wohlfarth, Philos. Trans. R. Soc. A **240**, 599 (1948).
[29] S. Khizroev, M. H. Kryder, Y. Ikeda, K. Rubin, P. Arnett, M. Best, D. A. Thompson, IEEE Trans. Magn. **35**, 2544 (1999).
[30] S. Khizroev, W. Jayasekara, J. A. Bain, R. E. Jones, Jr., M. H. Kryder, IEEE Trans. Magn. **34**, 2030 (1998).
[31] W. P. Jayasekara, S. Khizroev, M. H. Kryder, W. Weresin, P. Kasiraj, Fleming, IEEE Trans. Magn. **35**, 613 (1999).
[32] D. Litvinov, M. H. Kryder, and S. Khizroev, J. Appl. Phys. **93**, 9155 (2003).
[33] S. Khizroev, A. Lyberatos, M. H. Kryder, and D. Litvinov, Jpn. J. Appl. Phys., Part 2 **41**, L758 (2002).
[34] M. Mallary, private communications, 1997.
[35] E. Svedberg, D. Litvinov, R. Gustafson, and S. Khizroev, J. Appl. Phys. **93**, 2828 (2003).
[36] R. E. Jones, Jr., Acta Mater. **46**, 3805 (1998).
[37] M. Mallary, A. Torabi, and M. Benakli, IEEE Trans. Magn. **38**, 1719 (2002).
[38] Y. Kanai, R. Matsubara, H. Wanabe, H. Muraoka, and Y. Nakamura, IEEE Trans. Magn. **39**, 1955 (2003).
[39] M. L. Mallary, S. C. Das, U.S. Patent No. Re.33949, June 2, 1992.